Combined phenomenon of transverse impedance and beam-beam interaction with large Piwinski angle

Yuan Zhang,[1,2,*] Na Wang,[1] Kazuhito Ohmi,[3,†] Demin Zhou,[3] Takuya Ishibashi,[3] and Chuntao Lin[4,‡]

[1]*Key Laboratory of Particle Acceleration Physics and Technology, Institute of High Energy Physics, Chinese Academy of Sciences, 19(B) Yuquan Road, Beijing 100049, China*
[2]*University of Chinese Academy of Sciences, Beijing 100049, China*
[3]*KEK, Tsukuba, Ibaraki 305-0801, Japan*
[4]*Institute of Advanced Science Facilities, Shenzhen, Guangdong, 518107, China*

(Received 10 January 2023; accepted 26 May 2023; published 12 June 2023)

The crab-waist scheme becomes the baseline for future circular e^+e^- colliders, where a large Piwinski angle is a must. It has been first found that a strong coherent head-tail instability in the vertical direction may be induced by the interplay of beam-beam interaction and ring impedance below the conventional transverse mode-coupling instability threshold. The collision would be stable only considering pure beam-beam interaction. That is to say, the new instability is a combined effect of beam-beam interaction and ring impedance. The instability can limit the performance of future colliders based on the crab-waist scheme. Mode analysis has been done to help understand the physics. Mitigation schemes are also presented and verified by analysis and simulation.

DOI: 10.1103/PhysRevAccelBeams.26.064401

I. INTRODUCTION

The crab-waist (CW) collision [1] scheme was proposed to boost the luminosity of a lepton collider and has been successfully demonstrated at DAΦNE [2]. The experimental results of DAΦNE show that the novel scheme increases the peak luminosity by a factor of 3 with respect to that achieved before the upgrade. The CW collision scheme consists of a large Piwinski angle, small vertical beta functions at the IP (i.e., β_y^*), and suppression of beam-beam resonances by sextupole pairs creating a "crab-waist" configuration [3].

The CW scheme has become the baseline design of SuperB, SuperCT, CEPC, and FCCee [4–8]. The initial design of SuperKEKB [9] adopted the "nanobeam" scheme (i.e., large Piwinski angle plus small β_y^*, but without crab waist sextupoles). Beam commissioning in SuperKEKB without the CW showed that the blowup of vertical beam sizes was uncontrollable [10]. In 2020, the FCCee-like CW scheme [11] was successfully introduced to SuperKEKB to suppress the vertical blowup. In 2022, a new luminosity record of 4.65×10^{34} cm^{-2} s^{-1} was achieved at SuperKEKB with CW collision [10].

During the design of FCCee, a coherent beam-beam head-tail instability (X-Z instability) has been revealed via beam-beam simulation [12] and later validated by the mode analysis method [13]. This X-Z instability has also been seen in beam-beam simulations for CEPC [14] and observed in machine studies at SuperKEKB [15]. This instability sets a new constraint on machine parameters and has greatly impacted the design of CEPC and FCCee.

In storage rings, the conventional longitudinal impedance causes potential-well distortion (PWD) and consequently modifies the synchrotron motion of particles inside a bunch. Since synchrotron motion plays an essential role in the X-Z instability driven by beam-beam interaction, this instability may be disturbed by PWD. The combined effects between beam-beam interaction and longitudinal impedance have been studied by numerical simulations and analysis method [16–18]. For CEPC CDR parameters, it has been found that there would not exist a large enough stable tune area when the effect of longitudinal impedance is considered. The related work has pushed the evolution of machine parameters and optics design of the two future machines, CEPC and FCCee [19]. These findings indicate that in the present and future colliders with crab waist and large crossing angles, different dynamic effects should be modeled self-consistently in simulations and/or analyses to ensure a reliable prediction of beam stability.

The X-Z instability driven by beam-beam interaction arises from the strong coupling between horizontal and

*zhangy@ihep.ac.cn
†ohmi@post.kek.jp
‡linchuntao@mail.iasf.ac.cn

longitudinal motions. It is a coherent head-tail instability and can be enhanced by longitudinal impedance. In principle, a vertical head-tail instability driven by the interplay of beam-beam and conventional impedance can also appear. Studies on the interplay of beam-beam interaction and transverse impedance in hadron colliders, such as LHC and Tevatron, were reported in the literature [20,21]. However, in e^+e^- colliders, there is a lack of investigations of such an interplay. Recently, strong-strong beam-beam simulations with vertical impedance showed that a σ head-tail instability may appear in CEPC and SuperKEKB [22,23]. The results showed that this vertical instability can appear below the transverse mode-coupling instability (TMCI) threshold (here, the TMCI threshold is determined by vertical impedance without collision). This paper extends the previous work and intends to present a detailed study of the interplay between beam-beam effects and vertical impedance in e^+e^- colliders.

The paper is organized as follows: In Sec. II, we introduce the vertical cross-wake force of beam-beam interaction as an extension of the horizontal case [12]. The fundamental formulations of the mode analysis method for studies of head-tail instabilities are also briefly reviewed. Using CEPC parameters, the combined effect of beam-beam interaction and vertical impedance is analyzed. Two schemes for mitigating this instability are also discussed based on the instability analysis. The results are shown in Sec. III. The simulation results for CEPC and SuperKEKB are documented in Sec. IV. In the end, the work is summarized, and more future work is discussed.

II. THEORETICAL MODEL

Conventionally, the concept of wakefield is used to describe the interaction of a single beam and its surroundings [24]. The wakefields exert a wake force on the beam and can drive collective instability. The beam-beam interaction is a phenomenon of two-beam effects. The beam-beam force can be treated as a cross-wake force, of which the impedance can be used in the mode analysis of beam instability. The horizontal cross-wake force of beam-beam interaction was introduced to study the coherent X-Z instability in Refs. [12,13]. This section formulates the vertical cross-wake force induced by beam-beam interaction and its application to the instability analysis method used in the paper.

A. Vertical cross-wake force

Equation (6) in Ref. [13] gave the cross-wake force in the horizontal plane. Following the notations of Kuroo *et al.*, the difference in the vertical momentum kicks with and without vertical centroid deviation $\Delta y_-/\Delta y_+$ can be expressed as

$$\begin{aligned}\Delta p_y^{(-)} &= \delta p_y^{(-)}(y_- + \Delta y_- - y_+ - \Delta y_+) - \delta p_y^{(-)}(y_- - y_+) \\ &= -\frac{N^{(+)}\rho^{(+)}(z')\delta z' r_e}{\gamma^{(-)}}[F_y(y_- - y_+ + \Delta y_- - \Delta y_+) \\ &\quad - F_y(y_- - y_+)] \\ &= -\frac{N^{(+)}\rho^{(+)}(z')\delta z' r_e}{\gamma^{(-)}}\frac{\partial F_y}{\partial y}\bigg|_{\substack{x=(z-z')\theta_c \\ y=y_- - y_+}}(\Delta y_- - \Delta y_+),\end{aligned} \tag{1}$$

where $N^{(+)}\rho^{(+)}(z')\delta z'$ is the number of particles contained in the $\delta z'$ of the e^+ bunch, $\gamma^{(-)}$ is the relativistic mass factor of the e^- bunch, θ_c is the half horizontal crossing angle, r_e is the classical radius of the electrons, and F_y is represented by the complex error function w as given in Eq. (4) in Ref. [13]

$$F = F_y + iF_x = \frac{2\sqrt{\pi}}{\Sigma}[w(A) - \exp(-B)w(C)], \tag{2}$$

where A, B, C are defined as

$$A = \frac{x + iy}{\Sigma}, \qquad B = \frac{x^2}{4\bar{\sigma}_x^2} + \frac{y^2}{4\bar{\sigma}_y^2}, \qquad C = \frac{\frac{\bar{\sigma}_y}{\bar{\sigma}_x}x + i\frac{\bar{\sigma}_x}{\bar{\sigma}_y}y}{\Sigma}, \tag{3}$$

with $\Sigma = 2\sqrt{\bar{\sigma}_x^2 - \bar{\sigma}_y^2}$ and $\bar{\sigma}_{x,y}^2 = (\sigma_{x,y}^{(+)2} + \sigma_{x,y}^{(-)2})/2$.

Therefore, the partial derivative of F with respect to y can be obtained as

$$\begin{aligned}\frac{\partial F}{\partial y} = \frac{2\sqrt{\pi}}{\Sigma}\Bigg\{&-\frac{2Ai}{\Sigma}w(A) - \frac{2}{\Sigma\sqrt{\pi}}\left[1 - \frac{\bar{\sigma}_x}{\bar{\sigma}_y}\exp(-B)\right] \\ &+ \left(\frac{y}{2\bar{\sigma}_y^2} + \frac{2i\bar{\sigma}_x}{\Sigma\bar{\sigma}_y}C\right)\exp(-B)w(C)\Bigg\}.\end{aligned} \tag{4}$$

Considering that, at the interaction point, the horizontal beam size is much larger than the vertical beam size, then we have $A = x/(2\bar{\sigma}_x)$, $B = A^2$, $C = 0$, $\Sigma = 2\bar{\sigma}_x$. If we further take $y = y_- - y_+ = 0$, $\partial F_y/\partial y$ can be simplified as

$$\begin{aligned}\frac{\partial F_y}{\partial y}\bigg|_{y=0} = \frac{\sqrt{\pi}}{\bar{\sigma}_x}\Bigg\{&\frac{x}{2\bar{\sigma}_x^2}\mathrm{Im}w\left(\frac{x}{2\bar{\sigma}_x}\right) \\ &+ \frac{1}{\sqrt{\pi}\bar{\sigma}_x}\left[-1 + \frac{\bar{\sigma}_x}{\bar{\sigma}_y}\exp\left(-\frac{x^2}{4\bar{\sigma}_x^2}\right)\right]\Bigg\}.\end{aligned} \tag{5}$$

The cross-wake force is defined as the differential of the beam-beam force as

$$W_y^{(-)}(z - z') = -\frac{N^{(+)}r_e}{\gamma^{(-)}}\frac{\partial F_y}{\partial y}\bigg|_{\substack{y=0 \\ x=(z-z')\theta_c}}. \tag{6}$$

Substituting Eq. (5) into Eq. (6), the vertical cross-wake force can be written as

$$W_y^{(-)}(z) = -\frac{N^{(+)} r_e}{\gamma^{(-)}} \frac{\sqrt{\pi}}{\bar{\sigma}_x} \left\{ \frac{\zeta}{2\bar{\sigma}_x} \mathrm{Im} w\left(\frac{\zeta}{2}\right) + \frac{1}{\sqrt{\pi}\bar{\sigma}_x} \left[-1 + \frac{\bar{\sigma}_x}{\bar{\sigma}_y} \exp\left(-\frac{\zeta^2}{4}\right) \right] \right\}, \quad (7)$$

where $\zeta = \theta_p z/\sigma_z$ and $\theta_p = \theta_c \bar{\sigma}_z/\bar{\sigma}_x$ is the Piwinski angle. With flat-beam approximation $\bar{\sigma}_y/\bar{\sigma}_x \ll 1$, the expression of $W_y^{(-)}$ can be well approximated by the leading term as

$$W_y^{(-)}(z) = -\frac{N^{(+)} r_e}{\gamma^{(-)}} \frac{1}{\bar{\sigma}_x \bar{\sigma}_y} \exp\left(-\frac{\zeta^2}{4}\right). \quad (8)$$

The cross-wake force $W_y^{(-)}(z)$ can be treated as a wake function. By definition, we can obtain the vertical beam-beam impedance as

$$Z_y(\omega) = i \int_{-\infty}^{\infty} W_y(z) e^{-i\omega z/c} \frac{dz}{c}, \quad (9)$$

where c is the speed of light.

As the collision proceeds from the head of the bunch to the tail, the total vertical momentum kicks of Eq. (1) can be expressed as the integration of the cross-wake force of Eq. (6),

$$\Delta p_y^{(\mp)}(z) = -\int_{-\infty}^{\infty} W_y^{(\mp)}(z-z') \rho_y^{(\pm)}(z') dz' + \int_{-\infty}^{\infty} W_y^{(\mp)}(z-z') \rho^{(\pm)}(z') dz' \Delta y^{(\mp)}(z), \quad (10)$$

where $\rho_y(z) = \rho(z) \cdot \Delta y(z)$. On the right side of the above equation, the first integral represents the dipole term, and the second is the quadrupole term in which the strength of the kick is proportional to the deviation $\Delta y^{(\mp)}(z)$ of itself.

For beam-beam interaction of symmetric beams, we can assume that the two colliding beams contain only a σ mode where the dipole moment distributions are identical $\rho_y^{(+)}(z) = \rho_y^{(-)}(z)$ or a π mode where the distributions are opposite $\rho_y^{(+)}(z) = -\rho_y^{(-)}(z)$. With this assumption, the momentum kicks of Eq. (10) of the two-beam can be reduced to a single-beam momentum kick,

$$\Delta p_y(z) = \mp \int_{-\infty}^{\infty} W_y(z-z') \rho_y(z') dz' + \int_{\infty}^{\infty} W_y(z-z') \rho(z') dz' \Delta y(z). \quad (11)$$

The first integral containing ρ_y is the dipole term, with the "−" sign for σ mode, and the "+" sign for π mode. The second integral is the quadrupole term, which is the same for both σ and π modes.

B. Mode analysis method

We use the method presented in Ref. [18] to treat the cross-wake force from beam-beam interaction for beam instability analysis. The wake force induced by conventional ring impedance could also be considered using the same method. The mode analysis method is briefly introduced in the following.

The dipole moments of the bunch in longitudinal phase space (J, ϕ) are normalized and expanded in terms of azimuthal modes,

$$\frac{y(J,\phi)}{\sqrt{\beta_y}} = \sum_{l=-\infty}^{\infty} y_l(J) e^{il\phi}, \qquad \sqrt{\beta_y} p_y(J,\phi) = \sum_{l=-\infty}^{\infty} p_l(J) e^{il\phi}, \quad (12)$$

where β_y is the vertical β function. Here we have assumed that the α function at IP is zero since the IP should be a pure waist point in a ring collider.

At the IP, the change of momentum due to dipole and quadrupole wakefields induced by the beam-beam interaction of Eq. (11) can be written as,

$$\Delta p_l(J) = \int dJ' \sum_{l'=-\infty}^{\infty} [\mp \beta_y^* W_{l,l'}(J,J') \psi(J') y_{l'}(J') + \beta_y^* V_{l,l'}(J,J') \psi(J') y_{l'}(J)], \quad (13)$$

where

$$W_{l,l'}(J,J') = \frac{1}{2\pi} \iint d\phi d\phi' W_y(z-z') e^{-il\phi + il'\phi'}, \quad (14)$$

$$V_{l,l'}(J,J') = \frac{1}{2\pi} \iint d\phi d\phi' W_y(z-z') e^{-i(l-l')\phi}. \quad (15)$$

Here $W_{l,l'}$ and $V_{l,l'}$ correspond to the dipole and quadrupole kick in Eq. (11), respectively, and the $\mp$ sign in Eq. (13) correspond to σ/π mode. The parameter β_y^* is the beta function at the IP. With the discretization of J in Eq. (13), $\sqrt{J_i} = i\Delta J$ $(i = 1, \ldots, n_J)$ and truncation of l to $\pm l_{\max}$, the equation of motion is written as follows:

$$\Delta p_l(J_j) = \sum_{j'=1}^{n_J} \sum_{l'=-l_{\max}}^{l_{\max}} M_{jl,j'l'} y_{l'}(J_{j'}), \quad (16)$$

where

$$M_{jl,j'l'} = \mp\beta_y^* W_{l,l'}(J_j, J_{j'})\psi(J_{j'})\Delta J_{j'} + \sum_{j''=1}^{n_J} \beta_y^* V_{l,l'}(J_j, J_{j''})\psi(J_{j''})\Delta J_{j''}\delta_{jj'}. \quad (17)$$

The transfer map of beam-beam interaction for the vector $[y_l(J), p_l(J)]$ at the IP is as follows:

$$M_W = \begin{pmatrix} 1 & 0 \\ M_{jl,j'l'} & 1 \end{pmatrix}. \quad (18)$$

Together with the transfer matrix for the arc section,

$$M_0 = e^{-i2\pi l\nu_s} \begin{pmatrix} \cos\mu_y & \sin\mu_y \\ -\sin\mu_y & \cos\mu_y \end{pmatrix}, \quad (19)$$

where $\mu_y = 2\pi\nu_y$ is the betatron phase advance for one revolution and ν_s is the synchrotron tune. The total transfer matrix for one revolution is $M_0 M_W$. Finally, the stability of the colliding beams is determined by the eigenvalues $\lambda' s$. When considering the conventional ring impedance, the corresponding kick map is also applied at the IP following the same form of cross-wake force while the wake function now is from ring impedance.

If there does not exist PWD in the longitudinal direction, that is to say, the Poincare plot of beam motion in the longitudinal phase space is elliptic, we have

$$z = \sqrt{2\beta_z J}\cos\phi, \qquad \delta = \sqrt{2J/\beta_z}\sin\phi. \quad (20)$$

We can rewrite $V_{l,l'}(J, J')$ and $W_{l,l'}(J, J')$ using the transverse impedance

$$W_{l,l'}(J, J') = i^{l-l'-1}\int d\omega Z_y(\omega) J_l\left(\frac{\omega r_z}{c}\right) J'_{l'}\left(\frac{\omega r'_z}{c}\right), \quad (21)$$

$$V_{l,l'}(J, J') = i^{l-l'-1}\int_{-\infty}^{\infty} d\omega Z_y(\omega) J_{l-l'}\left(\frac{\omega r_z}{c}\right) J_0\left(\frac{\omega r'_z}{c}\right), \quad (22)$$

where $r_z = \sqrt{2\beta_z J}$, $z = r_z\cos\phi$, and J_l is the Bessel function.

Mode coupling may be induced if the off-diagonal matrix elements are nonzero. The wake function does not satisfy causality for the beam-beam cross-wake force since it is symmetric for z. The corresponding impedance is purely imaginary and symmetric for ω. $W_{l,l'}$, which is related to the dipole term, is zero for the opposite parity of l and l' (even-odd or odd-even). That is to say, there does not exist coupling between modes with different parities. While for the conventional wakefields, the causality is satisfied, and the wake function is 0 for $z > 0$. The corresponding wake has a finite real part and can induce mode coupling between all modes.

III. INSTABILITY ANALYSIS

Using the formulations of cross-wake force and mode analysis described in Sec. II, instability analysis can be performed with the input of machine parameters. The instability analysis provides a qualitative picture of the underlying physics in the combined effect of beam-beam interaction and conventional impedance. Here we use CEPC as an example of instability analysis, where the machine parameters are listed in Table. I. With the beamstrahlung bunch length and the ring impedance, the estimated TMCI threshold of the bunch population is approximately 21×10^{10}. That is to say, there does not exist conventional TMCI instability for the design bunch population considering the lengthened bunch due to beamstrahlung.

A. Cross-wake impedance at CEPC

Using the CEPC parameters, the beam-beam cross-wake functions weighted by the β functions at the IP are calculated and compared in Fig. 1. One can see that the amplitudes of the horizontal and vertical cross-wake functions are comparable. The beam-beam impedance is calculated from the wake function and compared with the conventional ring impedance in Fig. 2. Here, the impedances have been weighted by the local β functions of the impedance sources. The beam-beam impedances in the horizontal and vertical planes show quite different features. Especially in the frequency range of the bunch spectrum, the vertical beam-beam impedance is dominant compared with the horizontal beam-beam impedance. The β function weighted beam-beam impedance is roughly 5 times higher than that of the imaginary part of ring impedance except in the very low-frequency region. The real part of ring impedance, which has been included in the following instability studies, is also shown in Fig. 2.

B. Mode analysis for CEPC

For the mode analysis, we consider particles within $\pm 3\sigma_z$ regions corresponding J from 0 to $J_{\max} \approx 4.5\epsilon_z$. J is

TABLE I. Machine parameters (CEPC).[a]

Parameter		CEPC-Z
Energy	$E_{+/-}$ (GeV)	45.5
Bunch population	N_0 (10^{10})	14
Emittance	$\epsilon_{x/y}$ (nm/pm)	0.27/1.4
Beta at IP	$\beta^*_{x/y}$ (m/mm)	0.13/0.9
Bunch length (SR/BS)	σ_z (mm)	2.5/9.6
Energy spread (SR/BS)	σ_p (10^{-4})	4.0/13.7
Synchrotron tune	ν_s	0.0176
Damping time	$\tau_{x,y}$ (turn)	4919
Piwinski angle	$\sigma_z\theta_c/\sigma_x$	26.7
Beam-beam parameter	$\xi_{x/y}$	0.0036/0.111

[a]SR: Only considering synchrotron radiation in the ring and without collision. BS: Collision with the beamstrahlung effect is also considered.

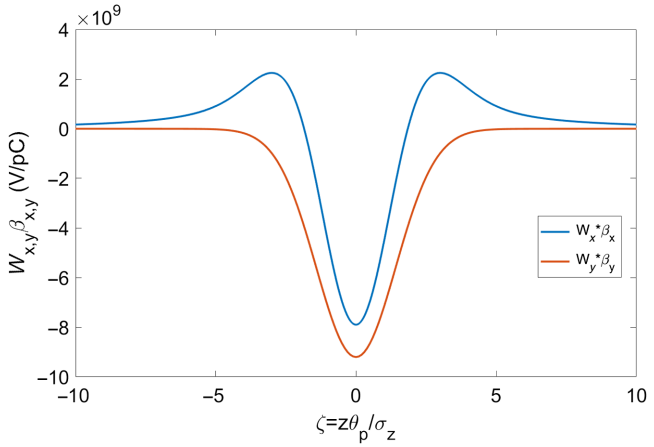

FIG. 1. Comparison of the horizontal and vertical beam-beam cross-wake function of CEPC which have been weighted by the local β functions at the IP.

discretized as $\sqrt{J_i} = i\Delta J, i = 1, \ldots, n_J$. We take the maximum mesh size as $n_J = 50$, and the maximum number of azimuthal modes as $l_{\max} = 13$ in the following calculation.

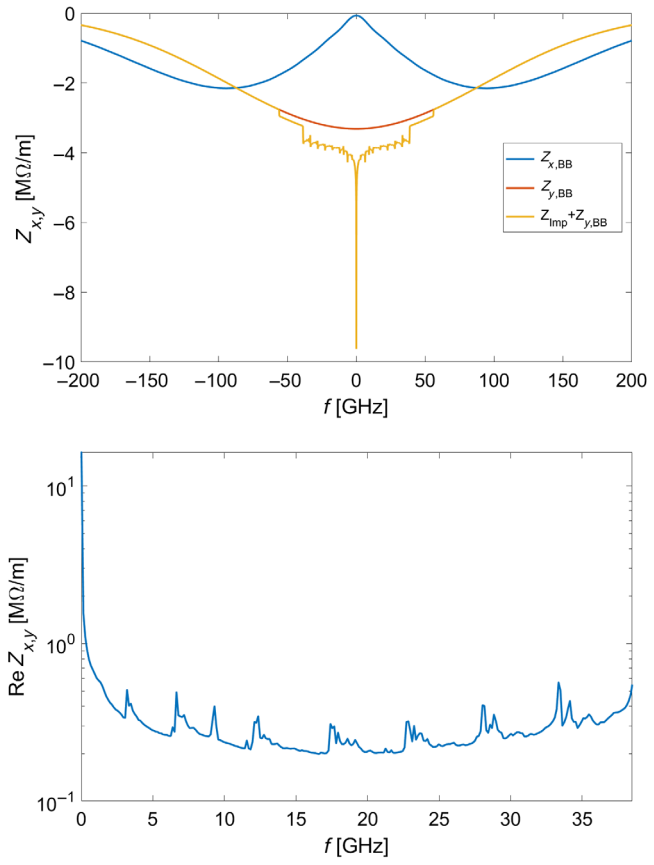

FIG. 2. Comparison of the CEPC ring impedance (imaginary part) with the horizontal and vertical beam-beam impedance (top), where the real part of the ring impedance (bottom) is also shown. The impedances have been weighted by the local β functions.

The momentum kick of conventional wakes is locally applied to the beam at IP, the same as treating the cross-wake force of beam-beam interaction. First, we ignore the quadrupole term in the beam-beam kick [see Eq. (11)] and clarify how the ring impedance influences the instability. Figure 3 compares the cases with and without ring impedance for the σ and π modes, respectively. Here the growth rate and eigentune are calculated by $\log\lambda$ and $\tan^{-1}(\mathrm{Im}\lambda/\mathrm{Re}\lambda)/(2\pi)$. To illustrate the underlying physics, we revisit the dipole term of the beam-beam cross-wake, which can be rewritten as

$$\Delta p_y(z) = \mp \int_{-\infty}^{\infty} W_y(z - z')\rho_y(z')dz', \tag{23}$$

where the $-$ and $+$ signs represent σ and π modes, respectively. Since $W_y < 0$ applies for any z, the dipole cross-wake force contributes a negative tune shift in σ mode and a positive one in π mode. For the wrapped modes [13], it is a positive tune shift in the σ mode and a negative one in the π mode. The instability would be induced when the modes of the same parity couple with each other. In the specific tune region, the σ mode would be much stronger than the π mode, which is similar to that in the horizontal direction as demonstrated in Ref. [13]. In fact, the cross-wake kick equation for σ mode is similar to that of ring wakefields. Since both the vertical cross-wake and ring wakefields are defocusing, the combination of two kinds of wakes is expected to enhance the σ mode instability. This is the case as shown in the upper subfigures of Fig. 3. At $\nu_y = 0.592$, there does not exist clear π mode instability as shown in the bottom subfigures of Fig. 3.

In the following, we consider both the dipole and quadrupole terms of the beam-beam kick. Quadrupole wakefield induced by monopole moment would not directly cause an exponential type of collective instability. The results for σ mode ($\nu_y = 0.592$) are shown in Fig. 4. It is seen that the instability is enhanced by ring impedance. Notably, the mode pattern is quite different from that without the quadrupole term, as shown in Fig. 3. Here the eigentunes are very dense with an increase in bunch current. This is because the vertical beam-beam tune shift is $\sim$0.1 for the design bunch population, which is much larger than that from the conventional TMCI case. The corresponding quadrupole term induces a large tune spread. Compared to Fig. 3, another impressive contribution from the quadrupole term is the reduction of instability growth rate, which is due to the Landau damping effect coming from the large tune spread.

It could be noticed in Fig. 4 that new unstable modes are induced near the bunch population $N = 0.2/0.5/0.8N_0$, where N_0 is the design one. They are induced by coupling between different azimuthal modes: $(-11, -1)$, $(-10, -2)$, $(-9, -3)$, $(-8, -4)$, $(-7, -5)$, $(-6, -6)$ near $0.2N_0$;

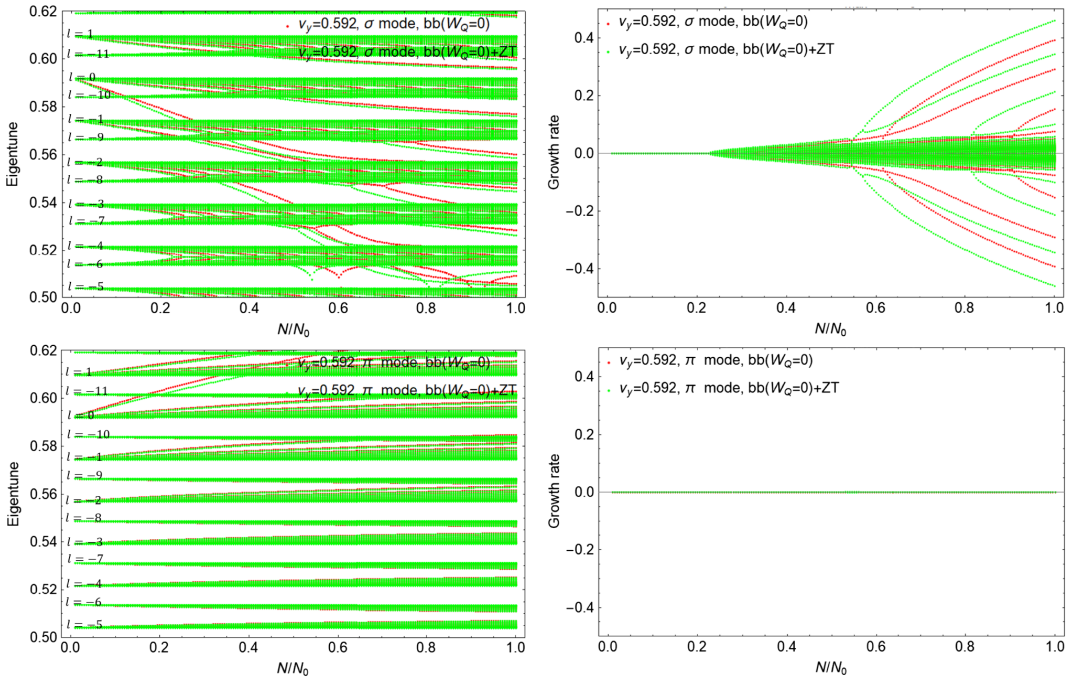

FIG. 3. Mode analysis of vertical oscillation versus bunch current for CEPC with vertical tune $\nu_y = 0.592$. The green and red dots in each subfigure indicate the cases with and without ring impedance, respectively. The above two figures are of σ mode. The below two figures are of π mode. Here only the dipole term of beam-beam kick is considered.

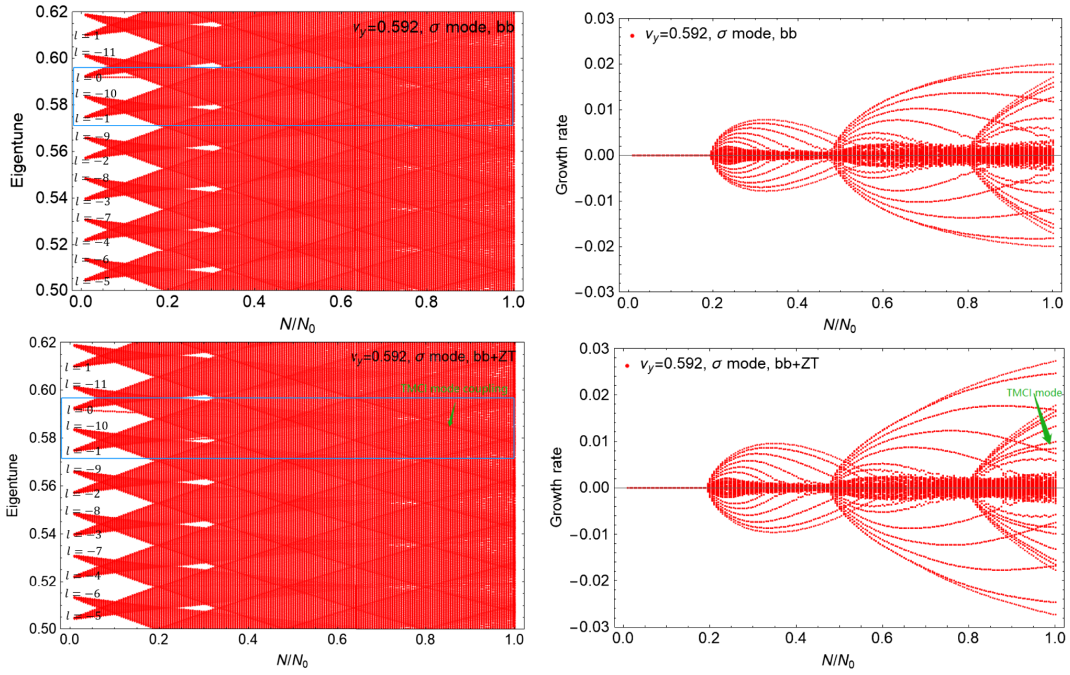

FIG. 4. Mode analysis of vertical oscillation versus bunch current ($\nu_y = 0.592$). The above two figures only consider beam-beam interaction. The below two figures consider both collision and ring impedance. The growth rate is faster with ring impedance.

$(-11,-3)$, $(-10,-4)$, $(-9,-5)$, $(-8,-6)$, $(-7,-7)$ near $0.5N_0$; $(-12,-4)$, $(-11,-5)$, $(-10,-6)$, $(-9,-7)$, $(-8,-8)$ near $0.8N_0$. It could be found that the coupling modes have high azimuthal modes. The unstable mode pattern is nearly kept unchanged with and without ring impedance, even the ring impedance really impacts the growth rate. The eigenvector of the most unstable mode at design bunch population N_0 is shown in Fig. 5. We can find

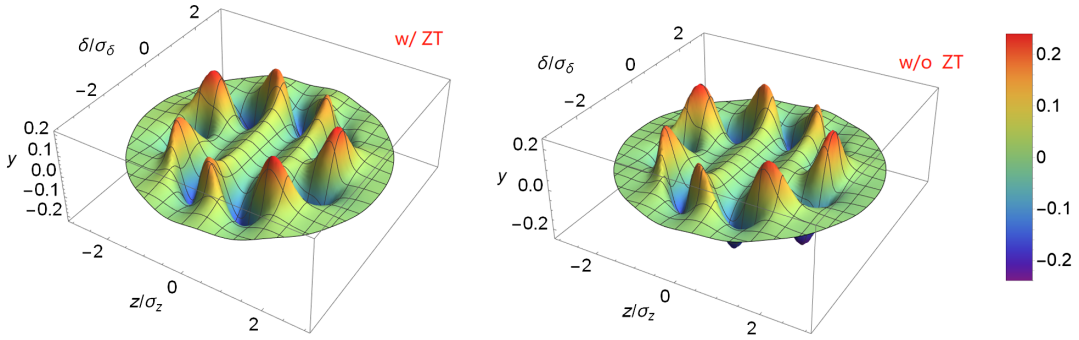

FIG. 5. Eigenvector of most unstable mode at design bunch population with (left) and without (right) ring impedance. y is an arbitrary unit.

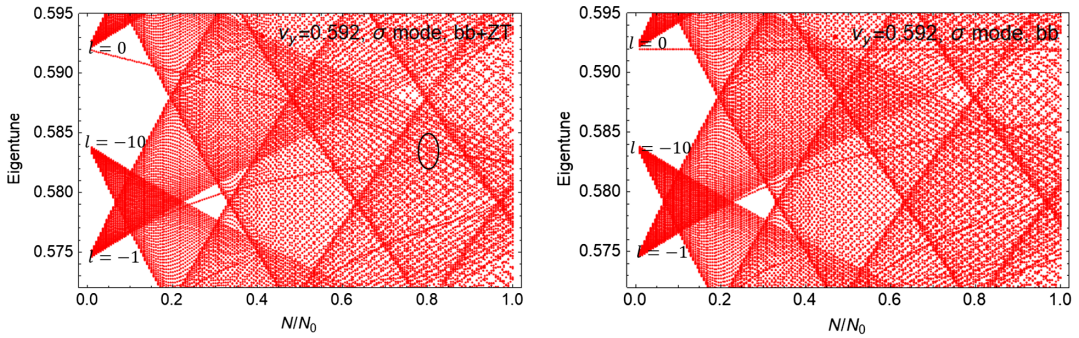

FIG. 6. Enlargement of the blue rectangular region in Fig. 4. Ring impedance is considered in the left figure, while not considered in the right figure.

that the ring impedance nearly does not change the eigenvector. There are seven peaks along the azimuthal which means the $l = 7$ modes dominate.

However, it is found that there really exist an unstable mode with low azimuthal mode number in case of that ring impedance is considered. It is induced by coupling between the 0 mode and -1 mode, which is identified in Fig. 4 and enlarged in Fig. 6. The zero mode ($l = 0$) tune would decrease with bunch population due to ring impedance, while -1 mode tune would increase with bunch population due to beam-beam interaction. The two modes would merge at lower bunch population than the conventional TMCI threshold. This specific unstable mode is called TMCI mode in the following. The eigenvector of the TMCI mode is also shown in Fig. 7, which is very similar to the conventional case. The eigenmode analysis with lower azimuthal modes ($l_{\max} = 4$) is also shown in Fig. 8 where no wrapped modes are included. Here only the TMCI mode appears and the results agree well with that shown in Figs. 4 and 6 ($l_{\max} = 13$). That is to say the TMCI mode is not related to the wrapped modes which are important to the X-Z instability.

Figure 9 shows the growth rate of σ/π mode instability versus vertical tune at design bunch population. Here both the dipole and quadrupole cross-wake forces are considered. Not only the most unstable mode but also the TMCI mode is shown for σ mode oscillation. The TMCI mode would be induced only when both beam-beam interaction and ring impedance are considered. The TMCI growth rate is not sensitive to the vertical tune, which is similar to the conventional case. It is noticed that the growth rate of the most unstable π mode is about one fourth of that σ mode. That is to say, the σ mode is expected to dominate the instability. The large tune spread by the quadrupole term also helps reduce the instability growth rate of π mode, while making the mode coupling easier to be induced together with the dipole term. That is why there does not exist stable tune considering the quadrupole term in π mode. It is clear

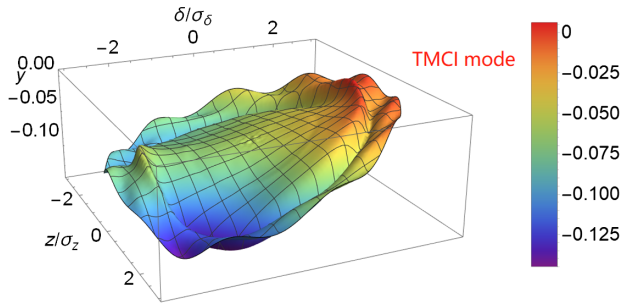

FIG. 7. Eigenvector of TMCI mode. y is an arbitrary unit.

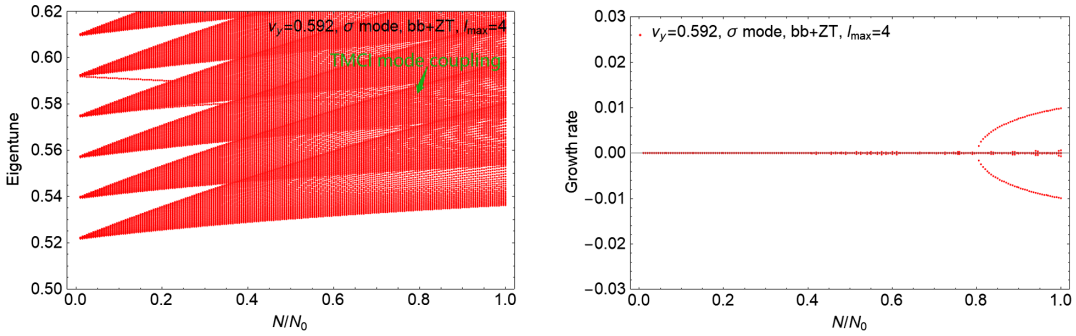

FIG. 8. The eigenmode analysis with lower azimuthal modes ($l_{\max} = 4$), where no wrapped modes are included.

that the π mode is not sensitive to the ring impedance, while the σ mode is very sensitive. Here we could also find that the σ mode instability is basically enhanced by the ring impedance. However, the π mode instability is more or less suppressed by ring impedance, which could be understood by referring to the above discussion only considering dipole wake.

We did not find any unstable eigenmode which is similar to the conventional TMCI instability for the π mode. Even the low azimuthal modes may couple, the radial distribution of the eigenvector of π mode is very singular (only appear in some specific narrow area of radial amplitude) and the corresponding growth rate is very low (< 0.001). These modes are supposed to be impossible to be induced in real case.

It is also noticed that the pure beam-beam interaction is even unstable, while it is stable in simulation. Since only the first-order derivative of beam-beam force is considered in the analysis, the instability is overestimated. Actually, the beam-beam force is evaluated only at the centroid in the analysis of this paper, while there are many particles with various betatron coordinates in a synchrotron phase space [25]. The coherent instabilities could be smeared out due to the nonlinear beam-beam force.

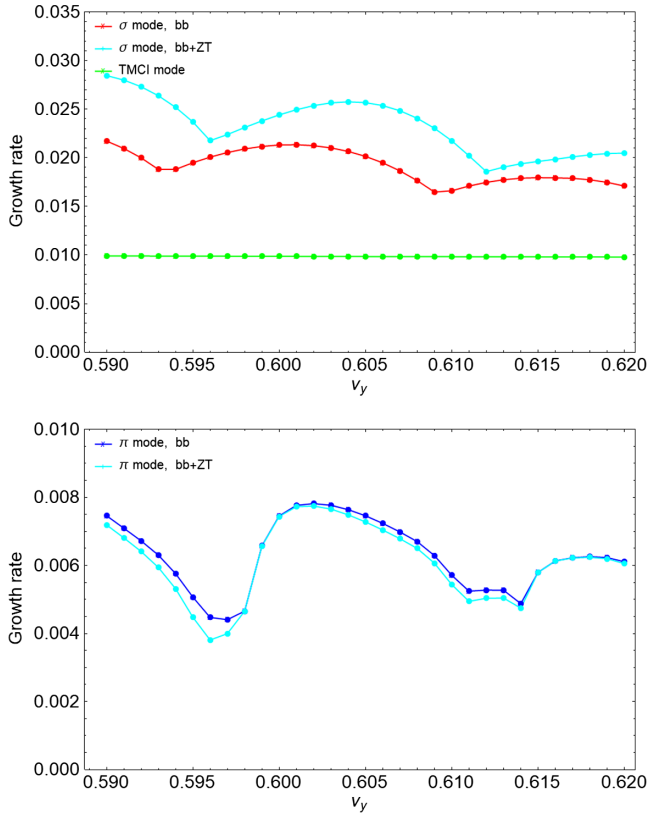

FIG. 9. The growth rate of σ/π mode versus vertical tune with the local beam-beam kick (BB) and ring impedance (ZT) at design bunch population. Besides the most unstable mode, the TMCI mode is also shown which only appears when ring impedance is considered.

C. Mitigation method

We first consider different betatron tunes for two colliding bunches since the σ mode dominates the instability and colliding bunches oscillate in phase. Then we study the effect of finite chromaticity, which is a classical method to suppress the TMCI instability.

1. Asymmetric tunes

Different from classical single-bunch instability, we are now studying the two-bunch instability occurring in the collision. It has been found that σ mode dominates the instability both in simulation and analysis. Different tunes for two beams are expected to help suppress the instability since they will not synchronize in phase. For this analysis study, we should deal with the two beams directly, and the matrix dimension is doubled than before. It is easy to extend the single-beam case (σ or π mode is assumed) to a two-beam case. Here we introduce it briefly.

The vector $(y_l^{(+)}(J), p_l^{(+)}(J), y_l^{(-)}(J), p_l^{(-)}(J))$ is transferred by M_0 in the arc section,

$$M_0 = \begin{pmatrix} M_0^{(+)} & 0 \\ 0 & M_0^{(-)} \end{pmatrix}, \tag{24}$$

where $M_0^{(\pm)}$ are transferred matrix for $e^{(\pm)}$ bunches in the arc section,

$$M_0^{(\pm)} = e^{-i2\pi l\nu_s^{(\pm)}} \begin{pmatrix} \cos\mu_y^{(\pm)} & \sin\mu_y^{(\pm)} \\ -\sin\mu_y^{(\pm)} & \cos\mu_y^{(\pm)} \end{pmatrix}. \quad (25)$$

At the IP, the transferred matrix M_W is expressed as follows:

$$M_W = \begin{pmatrix} 1 & 0 & 0 & 0 \\ \overline{V}^{(+)}_{jl,j'l'} & 1 & \overline{W}^{(+)}_{klk'l'} & 0 \\ 0 & 0 & 1 & 0 \\ \overline{W}^{(-)}_{klk'l'} & 0 & \overline{V}^{(-)}_{jl,j'l'} & 1 \end{pmatrix}, \quad (26)$$

where $\overline{W}^{(\pm)}_{jl,j'l'}, \overline{V}^{(\pm)}_{jl,j'l'}$ is defined as follows:

$$\overline{W}^{(\pm)}_{jl,j'l'} = -\sqrt{\beta_y^{*(+)}\beta_y^{*(-)}} W_{l,l'}(J_j^{(\pm)}, J_{j'}^{(\mp)})\psi(J_{j'}^{(\mp)})\Delta J_{j'}^{(\mp)}, \quad (27)$$

$$\overline{V}^{(\pm)}_{jl,j'l'} = \sum_{j''=1}^{n_J} \beta_y^{*(\pm)} V_{l,l'}(J_j^{(\pm)}, J_{j''}^{(\mp)})\psi(J_{j''}^{(\mp)})\Delta J_{j''}^{(\mp)}\delta_{jj'}. \quad (28)$$

Finally, the stability of the two colliding beams is determined by the eigenvalues λs of $M_0 M_W$.

Figure 10 shows the comparison of instability growth rate between symmetric and asymmetric tunes. Both the most unstable mode and TMCI mode are shown. The mitigation effect on the most unstable mode would be clear when the tune gap of two colliding bunches is greater than about 0.01. The TMCI mode suppression needs a larger tune difference.

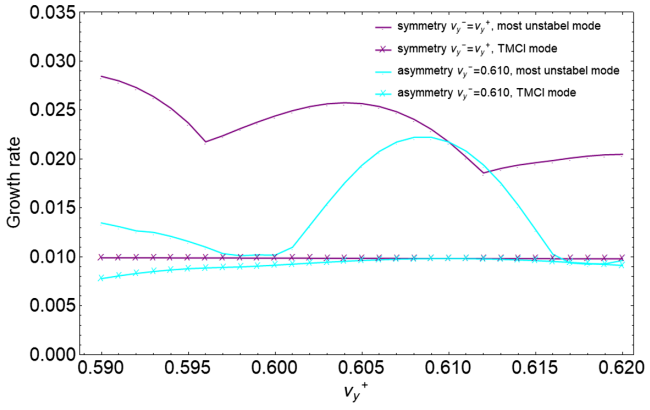

FIG. 10. Growth rate of vertical instability versus tune in case of symmetric and asymmetric tunes. In the asymmetric case, one beam's vertical tune is fixed at 0.61, and the other beam's vertical tune is scanned. For the symmetric case, the two beams' vertical tunes are the same and scanned together. Ring impedance is considered.

2. Chromaticity

We consider only linear tune chromaticity, and the betatron tune $\nu_y(\delta)$ is given by

$$\nu_y(\delta) = \nu_{y0} + \nu'_y\delta, \quad (29)$$

where ν_{y0} is the bare tune and ν'_y is the vertical tune chromaticity. Using the relation $\delta = \sqrt{2J/\beta_z}\sin\phi$ and $\phi(t) = \phi_0 + 2\pi\nu_s t$, the chromatic betatron phase advance for one turn is represented by

$$\begin{aligned}\mu_y(J,\phi) &= 2\pi\int_0^1 dt(\nu_{y0} + \nu'_y\sqrt{2J/\beta_z}\sin\phi) \\ &= 2\pi\nu_{y0} - \nu'_y\sqrt{2J/\beta_z}/\nu_s(\cos(\phi + 2\pi\nu_s) \\ &\quad - \cos\phi). \end{aligned} \quad (30)$$

For simplicity, we have replaced ϕ_0 by ϕ. Thus, the transformation of azimuthal modes in the arc section can be written as

$$\begin{aligned}\bar{x}_l(J) + i\bar{p}_l(J) = \frac{1}{2\pi}e^{-i2\pi l\nu_s}\sum_{l'=-l_{\max}}^{l_{\max}}[(x_{l'}(J) + ip_{l'}(J)) \\ \cdot\int_0^{2\pi} d\phi e^{-i(\mu_y(J,\phi)+(l-l')\phi)}], \end{aligned} \quad (31)$$

or

$$\begin{aligned}\bar{x}_l(J) &= \frac{1}{2\pi}e^{-i2\pi l\nu_s}\sum_{l'=-l_{\max}}^{l_{\max}}(A_{ll'}(J)x_{l'}(J) + B_{ll'}(J)p_{l'}(J)), \\ \bar{p}_l(J) &= \frac{1}{2\pi}e^{-i2\pi l\nu_s}\sum_{l'=-l_{\max}}^{l_{\max}}[-B_{ll'}(J)x_{l'}(J) + A_{ll'}(J)p_{l'}(J)], \end{aligned} \quad (32)$$

where

$$A_{ll'}(J) = \mathrm{Re}\left(\int_0^{2\pi} d\phi e^{-i(\mu_y(J,\phi)+(l-l')\phi)}\right), \quad (33)$$

$$B_{ll'}(J) = \mathrm{Im}\left(\int_0^{2\pi} d\phi e^{-i(\mu_y(J,\phi)+(l-l')\phi)}\right). \quad (34)$$

The transformation at the IP is the same as Eq. (18).

Figure 11 shows the instability growth rate with different vertical tune chromaticity by analysis. Both the most unstable mode and TMCI mode are shown. It is found that the instability could be mitigated clearly with large enough chromaticity. In the CEPC case, it is found that $\nu'_y \gtrsim 5$ is a must to weaken the combined instability of beam-beam interaction and ring impedance. Even the most unstable mode could not be suppressed totally, the TMCI

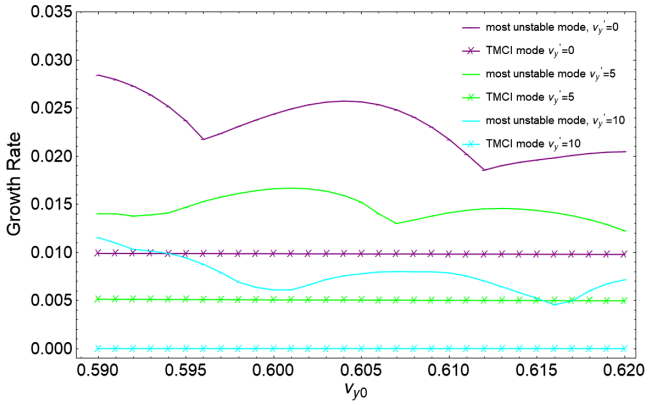

FIG. 11. The growth rate of vertical σ-mode instability with finite chromaticity considering both beam-beam interaction and ring impedance at different tunes.

mode could be well suppressed with $\nu_y' = 10$. Since the vertical tune is far from half integer, the large chromaticity is more or less acceptable.

IV. SIMULATION

Weak-strong beam-beam codes are unsuitable for this study since the coherent beam-beam instability could not appear in this model. Two independent strong-strong codes are used, and it is not found there exists any clear difference [26,27]. So in the following, we would not clarify which code is used for the specific result. In the horizontal direction, the localized beam-beam kick could induce the X-Z instability even without ring impedance. However, in the vertical direction, no coherent instability is found in the strong-strong simulation without ring impedance. Vertical instability can only be observed if ring impedance is considered. This section presents the simulation results at CEPC and SuperKEKB separately.

A. CEPC

In the simulations, both longitudinal and transverse impedances are considered. The longitudinal wakefield kick is applied at the IP, while the transverse one is applied evenly along the ring (64 kicks in the arc). There is no clear difference between 1 kick at IP and 64 kicks in the arc for transverse wakefield. The machine parameters are listed in Table I, and it is assumed the colliding beam parameters are symmetrical by default in CEPC.

We first ignore the vertical ring impedance and fix the vertical tune at $\nu_y = 0.61$. The horizontal tune is scanned to find a properly stable tune region to suppress the X-Z instability. We fix the horizontal tune at $\nu_x = 0.567$ to ensure X-Z instability does not exist. The vertical tune is then scanned considering vertical impedance. The result shows that there does not exist a stable tune area. Figure 12 shows the evolution of the vertical centroid

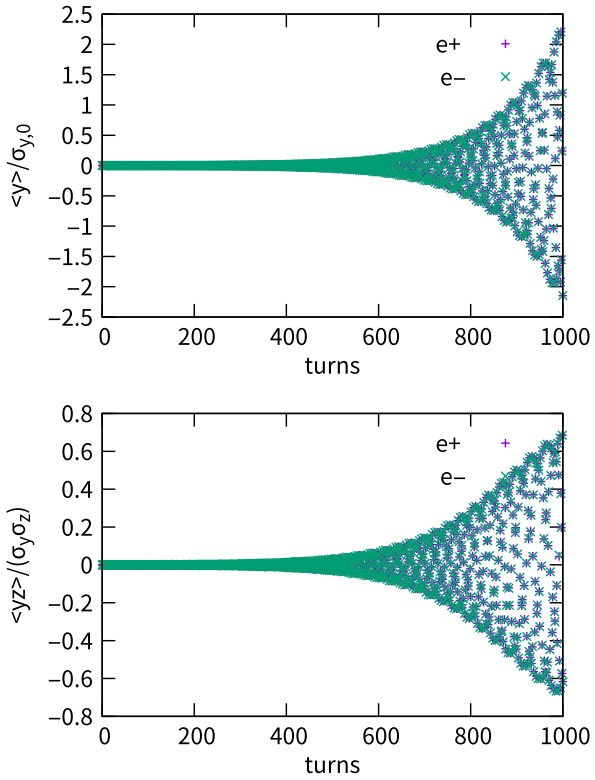

FIG. 12. Evolution of $\langle y \rangle$ and $\langle yz \rangle$ during a collision at $\nu_x/\nu_y = 0.567/0.61$ with vertical impedance.

and skew moment $\langle yz \rangle$ during the collision. It is clear that the colliding bunches oscillate in phase, which is the σ-mode instability. There also exists $\langle yz \rangle$ oscillation, which shows that it is a head-tail-like instability. The more detailed intrabunch dipole moment distribution is also checked, where $\langle y \rangle$ in longitudinal phase space is shown in Fig. 13. The results agree well with the eigenvector of TMCI mode (see Fig. 7) found in the analysis. Other high order modes found in analysis have never been seen in our simulation. It could be understood that high order modes would be mitigated by strong beam-beam nonlinearity. The instability in the vertical direction is different from X-Z instability. The vertical one is similar to the conventional TMCI instability, while the X-Z instability is induced by the wrapped modes coupling [13]. As mentioned before, the bunch population is below the single-bunch TMCI threshold where beamstrahlung length is used. Pure beam-beam interaction also does not induce any instability where ring impedance is not considered. That is to say, the new instability is a combined effect of beam-beam interaction and ring impedance, while the X-Z instability could be induced by pure beam-beam interaction. This vertical instability has never been found before in e^+/e^- colliders. It is not found that the crab-waist has a clear effect on the instability except that vertical beam size blowup due to nonoptimized crab-waist strength would impact the growth rate.

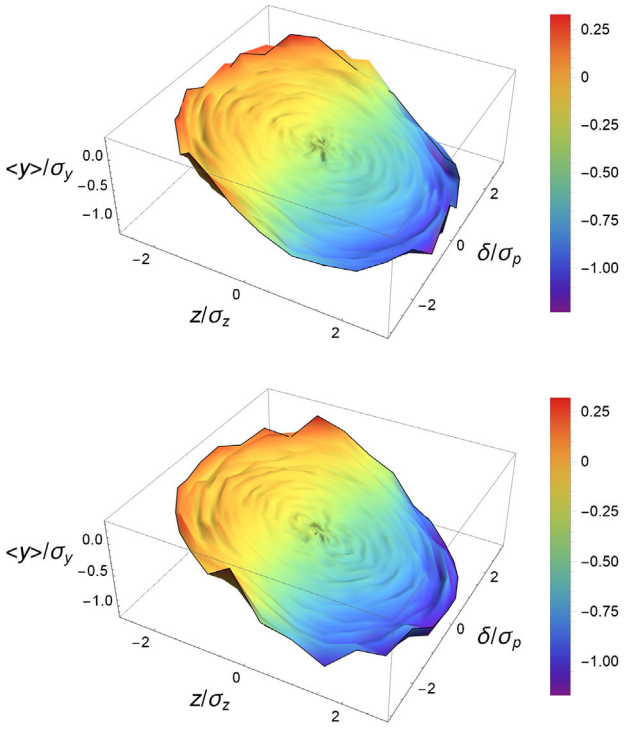

FIG. 13. Vertical centroid of two bunches in longitudinal phase space at the same turn. $z > 0$ is the head direction for two bunches.

In order to identify the impact of beamstrahlung on the instability, we compare the growth rate with and without beamstrahlung, where we keep the bunch length and energy spread, respectively, same in two cases. It is found that the beamstrahlung would help damping the instability a little, as shown in Fig. 14. The effect of beamstrahlung on vertical instability is different from that of X-Z instability. In the horizontal case, the instability is enhanced by the beamstrahlung effect [17]. It is supposed that this is due to the beamstrahlung effect being sensitive to horizontal beam

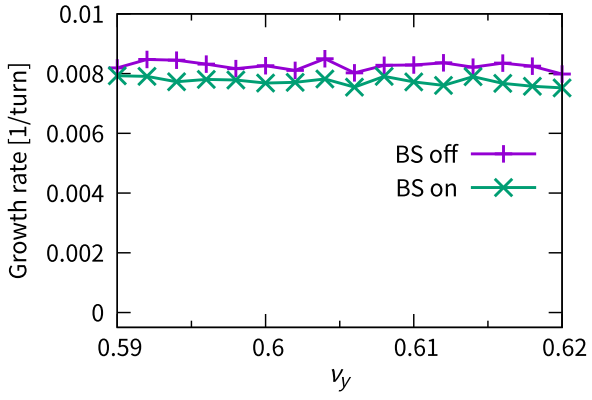

FIG. 14. Growth rate of vertical centroid versus tune with and without beamstrahlung effect. Both transverse and longitudinal impedances are considered.

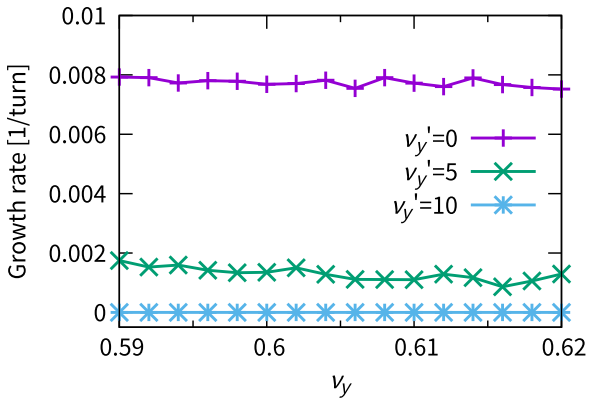

FIG. 15. Growth rate of vertical centroid versus tune with different vertical chromaticity. Both transverse and longitudinal impedance are considered.

size instead of vertical one [28]. However, the vertical beam size blowup may be very large ($\gtrsim$100) in simulation with beamstrahlung since X-Z instability may be induced after the vertical instability and vertical beam-beam interaction is enhanced thereafter [23].

To suppress the instability, one method is to use finite-tune chromaticity. The tune scan result with different tune chromaticity as shown in Fig. 15, where the transverse and longitudinal impedance is both considered. It could be found that the finite-tune chromaticity effectively mitigates the instability, even though the value must be large enough ($\nu_y' \sim 10$ in the CEPC case). The simulation results show good agreement with our analysis study. Tune chromaticity has also been used to mitigate the X-Z instability [29], where the transverse impedance is not considered.

Since the analysis and simulation show that the instability is σ mode, different working points between colliding beams may help mitigate the instability. We keep one beam's vertical tune fixed at 0.610 and scan the other one's. The result is shown in Fig. 16. It could be found that asymmetrical tunes could help mitigate the instability, which agrees well with analytical results. The chromaticity could be reduced from 10 to about 5 with different working points.

B. SuperKEKB

The machine parameters are listed in Table II. Here only the transverse impedance of LER is considered since the transverse impedance of LER is stronger than that of HER. The vertical impedance in LER is mainly contributed by the vertical collimators with small gaps. In our simulation, we put the transverse impedance at the D06V1 collimator, which is located in the injection region. The single bunch TMCI threshold is about 2 times higher than the bunch population used here.

The betatron tunes are optimized near (0.530,0.572) for HER and (0.525,0.589) for LER, respectively [30].

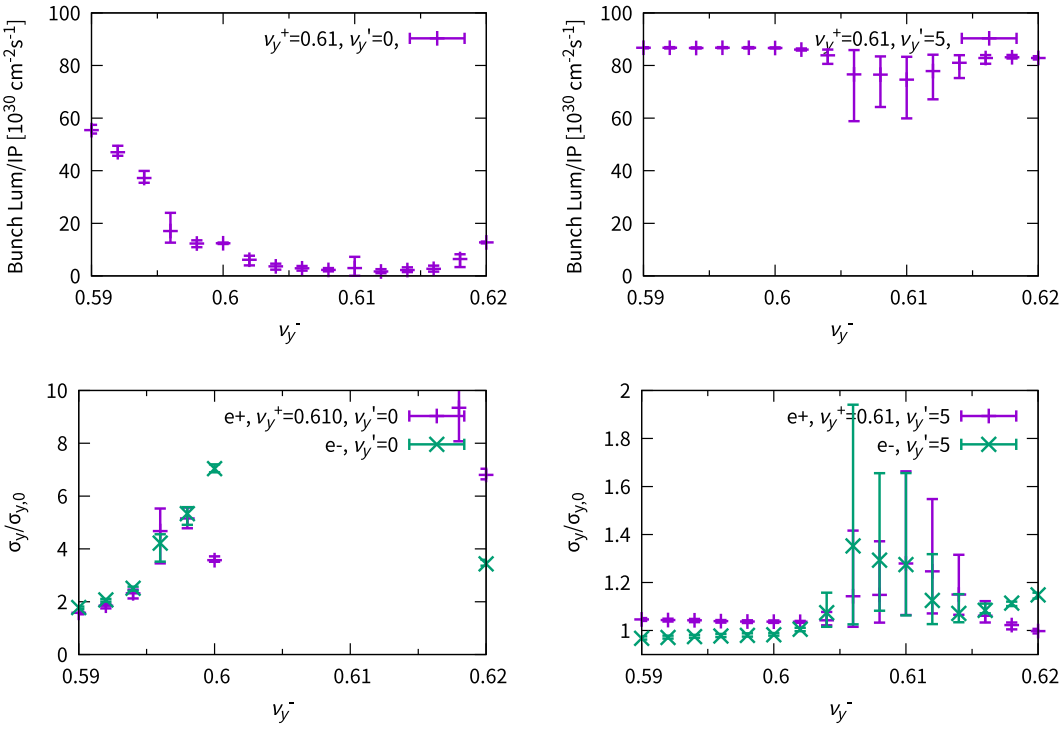

FIG. 16. Luminosity and vertical beam size versus asymmetric vertical tunes with different vertical chromaticity. Both transverse and longitudinal impedance are considered. One beam's vertical working point is fixed at 0.610.

The X-Z instability is well suppressed at the working points. The vertical tune scan of LER is shown in Fig. 17. Once the transverse impedance of LER is considered, there would exist strong vertical beam blowups in some specific tune regions. The turn-by-turn evolution shows that it is a σ-mode instability. There exists exponential growth of both dipole and quadrupole moment in the vertical direction, which is a TMCI-like typical phenomenon. A skew moment $\langle yz \rangle$ oscillation also exists, which shows a head-tail motion. It is more unstable when the colliding bunches' vertical tunes are closer since σ mode dominates. The phenomenon at SuperKEKB is very similar to that of CEPC, even though only LER's ring impedance is considered here.

TABLE II. Machine parameters (SuperKEKB).

	HER	LER
Energy (GeV)	7	4
Bunch population (10^{10})	5.02	6.28
Emittance x/y (nm/pm)	4.6/35	4.0/20
Beta at IP x/y (m/mm)	0.06/1	0.08/1
Bunch length (mm)	5.05	4.60
Energy spread (10^{-4})	6.3	7.5
Synchrotron tune	0.0272	0.0233
Damping time x (turn)	5760	4539

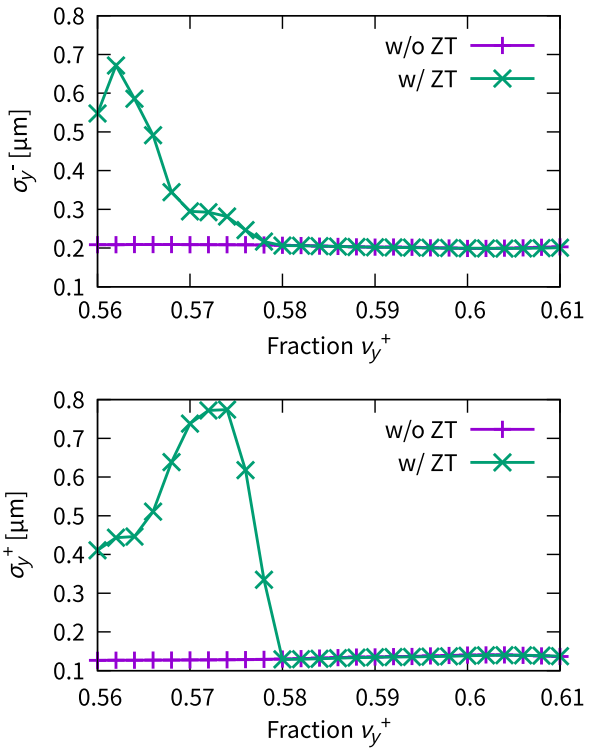

FIG. 17. Colliding beam size versus LER vertical tune with and without transverse impedance at SuperKEKB. The vertical tune of HER is fixed at 0.572.

V. SUMMARY AND OUTLOOK

It has been first found in simulation and analysis that the combined effects of beam-beam and transverse wakefields may induce TMCI-like instability in the modern e^+e^- ring colliders with large Pinwinski angle.

The combined phenomenon is studied by analysis and simulation. For the analysis, the vertical cross-wake force model is first built. The σ-mode instability in the analysis is stronger than that of π mode, and the latter one is not sensitive to the ring impedance. In our simulation, only σ-mode instability appears, which agrees with the analysis results.

When wrapped modes are considered, the analysis shows that pure beam-beam interaction would induce instability with high azimuthal mode. And the instability would be enhanced by ring impedance. The analysis also shows that there exists an unstable mode (TMCI) which is induced by the merge of 0 mode and -1 mode when ring impedance is considered, whether or not the wrapped modes are considered. That is to say the localized property of beam-beam force is not important for the TMCI mode. It is similar to the case of conventional TMCI instability. The 0 mode tune would decrease with bunch population due to ring impedance, while the -1 mode tune would increase due to cross-wake impedance. That is to say, the TMCI threshold would reduce when both beam-beam interaction and ring impedance are considered. In the π-mode analysis, we did not find any unstable mode similar to TMCI. The simulation shows that vertical instability could be induced in CEPC and SuperKEKB when the ring impedance is considered. The simulated results agree well with the TMCI mode found in the analysis. It seems the high azimuthal mode instability shown in the analysis is suppressed due to beam-beam nonlinearity since the analysis only considers the first-order beam-beam force.

Both analysis and simulation show that a large enough tune chromaticity could also help mitigate the serious instability. Another idea to mitigate the instability is to use asymmetric working points for colliding bunches since it is a σ-mode instability where two bunches oscillate in phase. The study shows that it is effective to weaken the instability with different working points. The choice of working point could not only consider beam-beam interaction, other cross-talk between beam-beam and lattice nonlinearity is also a complicated issue. This is beyond the scope of the paper. Since high-performance beam-beam collision is always pursued and the combined effect induces new instability, the impedance budget should be well constrained. A new nonlinear collimator [10] at SuperKEKB could help weaken the instability since it is expected to reduce the impedance. The design of CEPC is still evolving and it could be expected that the ring impedance would increase after more components are considered. The design optimization and instability mitigation need more work in the future. More measures, such as using a feedback system [31], to suppress the instability are future study.

In this paper, we studied the specific cases of CEPC and SuperKEKB, which both have large Piwinski angle. A question is how the instability would vary with the Piwinski angle. It is believed that the cross-impedance model would apply to different Piwinski angles. In fact, the instability studied in this paper is similar to physics as that of LHC [20] except their very different parameters. A more general study on the coherent beam-beam instability for different collision schemes (head-on, small and large Piwinski angle) will be presented in other paper.

In this paper, we focus on the vertical direction since the combined phenomenon is not significant in the horizontal direction. As we have learned, a modern (future) e^+e^- collider is much more challenging and complicated than before. The interplay between beam-beam and other dynamic effects must be considered in designing and commissioning high-performance e^+e^- colliders.

ACKNOWLEDGMENTS

The first author would like to thank M. Zobov, M. Migliorati, K. Oide, and D. Shatilov for fruitful discussions. The work is supported by the National Natural Science Foundation of China (Grant No. 12175249), the Chinese Academy of Sciences Visiting Professorship for Senior International Scientists (Grant No. 2019VMA0034), and Innovation Study of IHEP.

[1] P. Raimondi, in *Proceedings of the 2nd Super B-Factory Workshop, Frascati* (2006), http://www.lnf.infn.it/conference/superb06/.

[2] M. Zobov *et al.*, Test of Crab-Waist Collisions at DAΦNE Factory, Phys. Rev. Lett. **104**, 174801 (2010).

[3] P. Raimondi, D. N. Shatilov, and M. Zobov, Beam-beam issues for colliding schemes with large Piwinski angle and crabbed waist, Technical Report No. LNF-07/003, 2007, https://arxiv.org/abs/physics/0702033.

[4] M. Baszczyk *et al.* (SuperB Collaboration), SuperB technical design report, Technical Report, 2013, https://arxiv.org/abs/1306.5655.

[5] D. A. Epifanov and SCTF Collaboration, Project of super Charm-Tau factory, Phys. At. Nucl. **83**, 944 (2020).

[6] Q. Luo, Future projects for the next generation Tau-Charm factories in China and Russia, in *Proceedings of 65th ICFA Advanced Beam Dynamics Workshop High Luminosity Circular e^+e^- Colliders, Frascati, Italy* (JACOW, Geneva, Switzerland, 2023), MOXAT0107.

[7] CEPC Study Group, CEPC Conceptual Design Report: Volume 1—Accelerator, arXiv:1809.00285.

[8] A. Abada *et al.* (FCC), FCC-ee: The Lepton Collider: Future Circular Collider Conceptual Design Report Volume 2, Eur. Phys. J. Spec. Top. **228**, 261 (2019).

[9] Y. Ohnishi *et al.*, Accelerator design at SuperKEKB, Prog. Theor. Exp. Phys. **2013**, 03A011 (2013).

[10] Y. Funakoshi *et al.*, The SuperKEKB has broken the world record of the luminosity, in *Proceedings of 13th*

International Particle Accelerator Conference, IPAC'22, Bangkok, Thailand (JACoW, Geneva, Switzerland, 2022), MOPLXGD1.

[11] K. Oide, M. Aiba, S. Aumon, M. Benedikt, A. Blondel, A. Bogomyagkov, M. Boscolo, H. Burkhardt, Y. Cai, A. Doblhammer *et al.*, Design of beam optics for the future circular collider e^+ e^- collider rings, Phys. Rev. Accel. Beams **19**, 111005 (2016).

[12] K. Ohmi, N. Kuroo, K. Oide, D. Zhou, and F. Zimmermann, Coherent Beam-Beam Instability in Collisions with a Large Crossing Angle, Phys. Rev. Lett. **119**, 134801 (2017).

[13] N. Kuroo, K. Ohmi, K. Oide, D. Zhou, and F. Zimmermann, Cross-wake force and correlated head-tail instability in beam-beam collisions with a large crossing angle, Phys. Rev. Accel. Beams **21**, 031002 (2018).

[14] N. Wang, Y. Zhang, Y. Liu, S. Tian, K. Ohmi, and C. Lin, Mitigation of coherent beam instabilities in CEPC, in *Proceedings of ICFA mini-Workshop on MCBI, Zermatt, Switzerland, 2019* (CERN, Geneva, 2019).

[15] K. Ohmi, D. El Khechen, K. Hirosawa, H. Koiso, and Y. Ohnishi, Benchmarking of simulations of coherent beam-beam instability with SuperKERKB measurement, in *Proceedings of 62nd ICFA Advanced Beam Dynamics Workshop on High Luminosity Circular e^+e^- Colliders, Hong Kong, China* (JACOW, Geneva, Switzerland, 2019), TUYBA01.

[16] D. Leshenok, S. Nikitin, Y. Zhang, and M. Zobov, Combined influence of beamstrahlung and coupling impedance on beam energy spread and length in future lepton colliders, Phys. Rev. Accel. Beams **23**, 101003 (2020).

[17] Y. Zhang, N. Wang, C. Lin, D. Wang, C. Yu, K. Ohmi, and M. Zobov, Self-consistent simulations of beam-beam interaction in future e^+ e^- circular colliders including beamstrahlung and longitudinal coupling impedance, Phys. Rev. Accel. Beams **23**, 104402 (2020).

[18] C. Lin, K. Ohmi, and Y. Zhang, Coupling effects of beam-beam interaction and longitudinal impedance, Phys. Rev. Accel. Beams **25**, 011001 (2022).

[19] M. Migliorati, E. Carideo, D. De Arcangelis, Y. Zhang, and M. Zobov, An interplay between beam-beam and beam coupling impedance effects in the Future Circular e^+ e^- Collider, Eur. Phys. J. Plus **136**, 1190 (2021).

[20] S. White, X. Buffat, N. Mounet, and T. Pieloni, Transverse mode coupling instability of colliding beams, Phys. Rev. ST Accel. Beams **17**, 041002 (2014).

[21] E. G. Stern, J. F. Amundson, P. G. Spentzouris, and A. A. Valishev, Fully 3D multiple beam dynamics processes simulation for the Fermilab tevatron, Phys. Rev. ST Accel. Beams **13**, 024401 (2010).

[22] Y. Zhang, in *Proceedings of the 1st CEPC International Accelerator Review Committee Meeting in 2022, Beijing, China, 2022* (2022).

[23] K. Ohmi and Y. Zhang, in *Proceedings of the 10th Meeting of SKEKB ITF Beam-Beam Sub-Group* (2022).

[24] A. W. Chao, *Lectures on Accelerator Physics* (World Scientific, Singapore, 2020).

[25] K. Ohmi and A. W. Chao, Combined phenomena of beam-beam and beam-electron cloud interactions in circular e^+ e^- colliders, Phys. Rev. ST Accel. Beams **5**, 101001 (2002).

[26] K. Ohmi, Simulation of beam-beam effects in a circular e^+e^- collider, Phys. Rev. E **62**, 7287 (2000).

[27] Y. Zhang, K. Ohmi, and L.-M. Chen, Simulation study of beam-beam effects, Phys. Rev. ST Accel. Beams **8**, 074402 (2005).

[28] A. Bogomyagkov, E. Levichev, and D. Shatilov, Beam-beam effects investigation and parameters optimization for a circular e^+e^- collider at very high energies, Phys. Rev. ST Accel. Beams **17**, 041004 (2014).

[29] M. Migliorati, C. Antuono, E. Carideo, Y. Zhang, and M. Zobov, Impedance modelling and collective effects in the Future Circular $e+e$ Collider with 4 IPs, EPJ Tech. Instrum. **9**, 10 (2022).

[30] D. Zhou, Y. Funakoshi, K. Ohmi, Y. Ohnishi, and Y. Zhang, Simulations and measurements of luminosity at SuperKEKB, in *Proceedings of 13th International Particle Accelerator Conference, IPAC'22, Bangkok, Thailand* (JACoW, Geneva, Switzerland, 2022), pp. 2011–2014.

[31] V. Danilov and E. Perevedentsev, Feedback system for elimination of the transverse mode coupling instability, Nucl. Instrum. Methods Phys. Res., Sect. A **391**, 77 (1997).